American Mineralogist, Volume 77, pages 495–506, 1992

Phosphate speciation in potassium aluminosilicate glasses

Hao Gan, Paul C. Hess
Department of Geological Sciences, Brown University, Providence, Rhode Island 02912, U.S.A.

Abstract

Parallel- and perpendicular-polarized Raman, MAS, and static ^{31}P NMR spectra were collected to investigate phosphate speciation in potassium aluminosilicate glasses. Phosphate speciation is critically dependent on the K/(K + Al) (K*) ratio. In peralkaline melts (K* = 0.75), a series of high-frequency Raman bands are assigned to phosphate structural units of different degrees of polymerization (from monomer to dimer). The ^{31}P NMR spectra confirm the assignments. The MAS and static ^{31}P NMR spectra indicate that P resides in an $AlPO_4$-type environment outside the tetrahedra (SiO_4)-K(AlO_4) network in peraluminous melts (K* = 0.35). AlOP bonds ($AlPO_4$ type) and KOP bonds (KPO_3 type) form the dominant structural units in subaluminous melts (K* = 0.5).

Introduction

Homogeneous redox equilibria and heterogeneous phase equilibria experiments demonstrate that the alkali-Al ratio is one of the most significant chemical parameters controlling the solution properties of highly charged cations in silica-rich melts (Gwinn and Hess, 1989; Ellison and Hess, 1988; Dickenson and Hess, 1981, 1986; Montel, 1986; Naski and Hess, 1985; Dickinson and Hess, 1985; Watson, 1979). Alkalis in molar excess of Al_2O_3, for example, sharply lower the activity coefficients of ZrO_2, TiO_2, SnO_2, Fe_2O_3, and P_2O_5 in both dry and H_2O-saturated rhyolite melts. Moreover, this peralkaline effect surely reduces activity coefficients of Nb_2O_5, As_2O_5, CrO_3, and MoO_3: Raman spectra of alkali silicate glasses doped with these oxides indicate that these oxides form strong complexes with alkalis and largely reside outside the silicate network (Ellison and Hess, 1989; Nelson et al., 1983; Verweij, 1981; Brawer and White, 1977).

In addition, certain components also show a peraluminous effect wherein the activity coefficient of a high field-strength cation is lowered in melts with Al_2O_3/K_2O (molar) greater than unity. This was demonstrated to be true for P by measuring the solubility of $LaPO_4$ (monazite structure) in $(K_2O,Al_2O_3)\cdot 4SiO_2$ melts with varying K/Al ratios (Ellison and Hess, 1988). The solubility of $LaPO_4$ is lowest in subaluminous compositions (K = Al moles) and increases with either an increasing or a decreasing K/Al ratio. Clearly, the existence of a peraluminous and peralkaline effect in P_2O_5-bearing silicate melts implies a complex solution behavior of P.

This has obvious implications in the geochemical evolution of natural magmas. For example, the high P_2O_5 contents of certain pegmatites relative to high silica rhyolites may be a consequence of the peraluminous composition of pegmatite (London, 1987). Also, crystal-liquid distribution coefficients for rare earth elements in metaluminous melts are sensitive to the P_2O_5 content (Ryerson and Hess, 1978). Redox ratios are also impacted: the addition of P_2O_5 to granitic melts decreases the Fe^{2+}/Fe^{3+} redox ratio in peraluminous melts but increases it in others (Gwinn and Hess, 1992; Dickenson and Hess, 1983). Small amounts of P_2O_5 lower the liquidus temperature of H_2O-saturated granitic melts (Wyllie and Tuttle, 1964) but widen the two liquid solvus in the leucite-fayalite-silica system (Visser and Koster van Groos, 1979; Watson, 1976). The solubility of phosphate is greatest in ultramafic melts and least in granitic melts under identical temperatures and pressures (Dickinson and Hess, 1983; Watson, 1979). It is imperative, therefore, to understand the structural role of P_2O_5 in silicate melts over a wide range of chemical and physical conditions. The purpose of this paper is to determine the homogeneous equilibria of P in anhydrous peralkaline and in subaluminous and peraluminous granitic melts, using a combination of Raman and NMR spectroscopy to analyze rapidly quenched P_2O_5-bearing glasses in the system SiO_2-Al_2O_3-K_2O.

Glass preparation and experimental methods

Glass compositions were synthesized in three different regions of the 80 mol% SiO_2 isopleth in the SiO_2-Al_2O_3-K_2O system (Table 1, Fig. 1), i.e., peralkaline [K* = K_2O/(K_2O + Al_2O_3) molar > 0.5] with K^+ in excess of Al^{3+}, peraluminous (K* < 0.5) with Al^{3+} in excess of K^+, and subaluminous (K* = 0.5) with equal amounts of K^+ and Al^{3+} cations. K* values of 0.75, 0.5, and 0.35 were chosen as representative for each region, and P_2O_5 contents varied from 0 to 8 mol% in peraluminous and subaluminous glasses and from 0 to about 3 mol% in peralkaline glasses. The low P_2O_5 contents of the peralkaline glasses are limited by crystallization and phase separation.

Most of the glasses were prepared by the Corning Glass

0003–004X/92/0506–0495$02.00

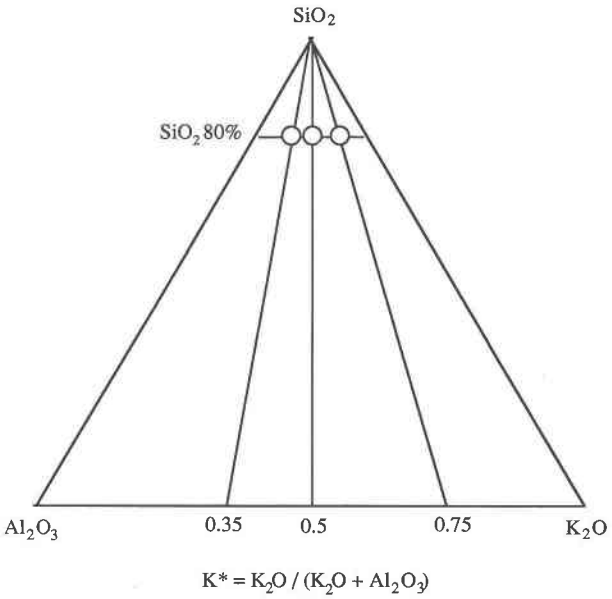

Fig. 1. Triangular plot of the glass compositions. All the points stand along 80 mol% SiO_2 isopleth.

Works. Batches of 500 g each were made by mixing appropriate ratios of reagent grade carbonate and oxides, then melted for 4–6 h at 1650–1800 °C. Melts were then quenched by rapidly pouring them into a cold steel plate. The glass of sample P3 was melted at 1550 °C and quenched in cold H_2O at Brown University.

In order to test the chemical compositions and homogeneity of the glasses, electron microprobe analyses were performed at Brown University with a Cameca Camebax (TM) electron microprobe, using a 15-kV accelerating potential, 10-nA beam current, and 25-μm beam diameter. Si, Al, K, and P were counted for 10 s each. Table 1 shows glass compositions determined by electron microprobe. K loss occurred in some samples during melting, but the compositions are still very close to the nominal values. The glasses were homogeneous in the scale of microprobe beam and free of crystals by XRD.

Raman spectra of glasses were collected with a Spex 1403 double monochrometer using the green light (514.5 nm) of a Spectra-Physics 263 Ar^+ laser. Entrance and exit spectral slit widths were adjusted to give a 3-cm^{-1} resolution. Parallel-polarized (HH) and perpendicular-polarized (HV) Raman spectra were obtained by rotating an analyzer placed between the sample and entrance port without varying sample position and laser intensity. Individual scans were collected at 2-cm^{-1} increments for scan times of 1 s/increment. A total of 20–70 scans were collected sequentially and summed together. All the spectra were then normalized to represent a sum of 45 scans. Each corresponding HH and HV spectrum has the same intensity at 1450 cm^{-1} because the background intensity of 1450 cm^{-1} is subtracted from each. Raman spectra of several crystalline potassium phosphates were collected from their powders in capillary tubes.

Most of the static and MAS ^{31}P NMR spectra were gathered on a Bruker MSL-300 spectrometer with a 7.1-T cryomagnet at Brown University. The resonance frequency is 121.5 MHz and the spinning rate is 5.0 KHz for MAS NMR. Pulses of 5.9 μs with a repetition time of 15–20 s and a delay time of 10–15 μs were used as the acquisition parameters. The static and MAS ^{31}P NMR spectrum of sample P3 was collected at the University of Illinois. The resonance frequency is 145.6 MHz and the spinning rate is 9.5 KHz for MAS NMR. An 85% aqueous solution of H_3PO_4 served as the ^{31}P spectrum reference. The increasing positive chemical shift corresponds to deshielded values. Figures showing stacked spectra in this paper (both Raman and NMR spectra) are drawn to show as many features as possible. Therefore, the intensity scales vary from sample to sample, and the comparisons are only valid within the same sample.

Raman spectra

The peralkaline glasses

Raman spectra of peralkaline glasses (nominal K* = 0.75) are given in Figure 2. For convenience, the spectra are divided into three separate regions: the high-frequency region above 800 cm^{-1}, the midfrequency region between 500 and 800 cm^{-1}, and the low-frequency region below 500 cm^{-1}.

In the high-frequency region (>800 cm^{-1}), P-free potassium aluminosilicate glass has a polarized band at 1090 cm^{-1} and a noticeable shoulder near 1150 cm^{-1} (see also Domine and Piriou, 1986). This is very similar to the

Table 1. Chemical compositions of the glasses

Samples	K*	SiO_2 (wt%)	Al_2O_3 (wt%)	K_2O (wt%)	P_2O_5 (wt%)	SiO_2 (mol%)	Al_2O_3 (mol%)	K_2O (mol%)	P_2O_5 (mol%)
P-3	0.78	69.2	5.7	19.7	5.4	79.1	3.9	14.4	2.6
P-9	0.73	69.9	7.4	19.2	3.5	79.5	4.9	13.9	1.7
P-11	0.68	71.5	9.8	19.2	0.0	79.9	6.5	13.7	0.0
P-6	0.34	59.9	17.3	8.1	15.5	73.2	12.5	6.3	8.0
P-7	0.33	66.0	18.5	8.5	7.9	77.1	12.7	6.3	3.9
P-12	0.29	65.7	22.6	8.7	4.1	76.1	15.4	6.5	2.0
P-8	0.33	71.5	20.6	9.2	0.0	79.9	13.6	6.5	0.0
P-4	0.48	60.6	13.2	11.4	15.0	73.9	9.5	8.9	7.7
P-5	0.49	65.3	14.4	12.6	8.0	76.7	9.9	9.4	4.0
P-13	0.49	68.9	15.0	13.2	3.4	78.6	10.1	9.6	1.7
P-10	0.50	70.1	15.8	14.7	0.0	79.0	10.5	10.6	0.0

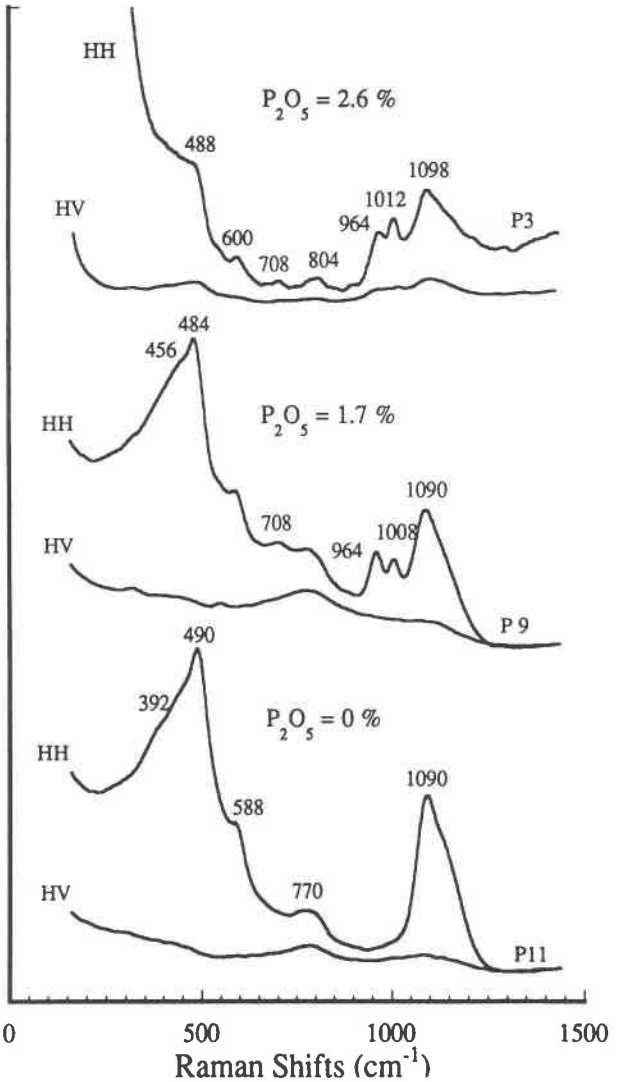

Fig. 2. The Raman spectra of peralkaline glasses. Top line is HH, bottom line is HV spectrum for each sample: P11 (P_2O_5 = 0%), P9 (P_2O_5 = 1.7%), P3 (P_2O_5 = 2.6%).

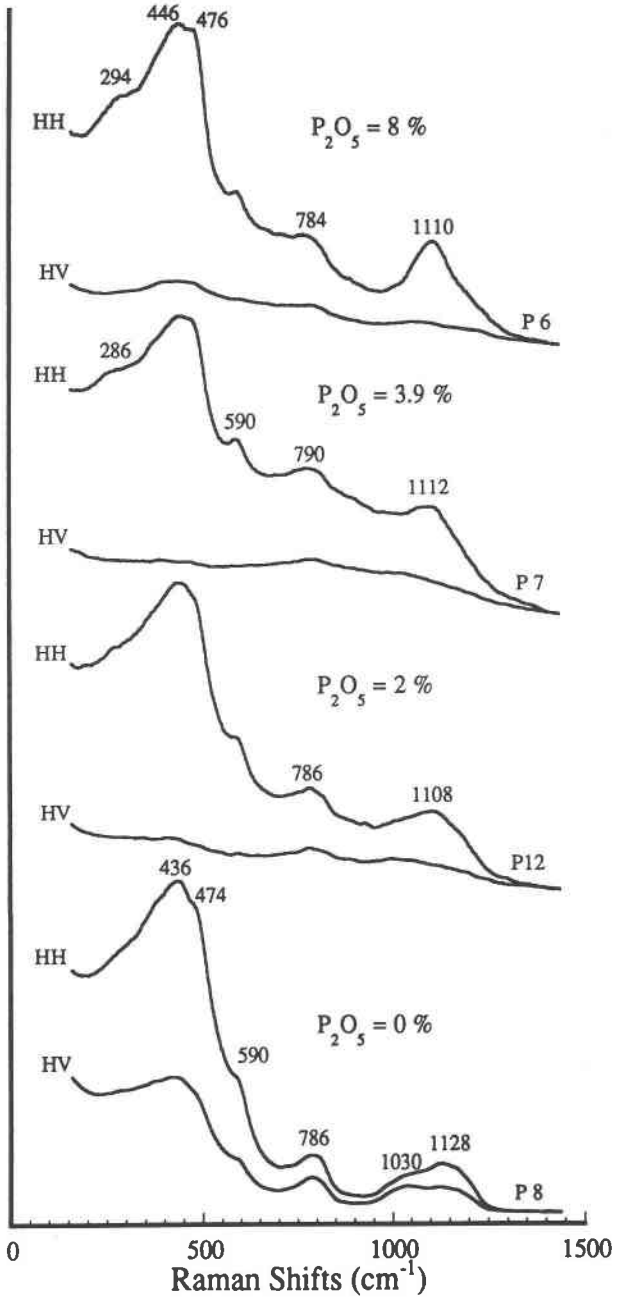

Fig. 3. The Raman spectra of peraluminous glasses. Samples P8 (P_2O_5 = 0%), P12 (P_2O_5 = 2%), P7 (P_2O_5 = 3.9%), P6 (P_2O_5 = 8%).

high-frequency bands in the spectra of K_2O-$n SiO_2$ glasses with $n > 2$ (Matson et al., 1983). The 1090-cm^{-1} and 1150-cm^{-1} bands are present also in the spectra of P_2O_5-bearing glasses, but their intensities relative to the 490-cm^{-1} bands decrease with increasing P_2O_5. In addition, two strongly polarized bands of roughly equal intensity appear at 964 and 1008 cm^{-1} in the glass with 1.7 mol% P_2O_5. The 1008-cm^{-1} band becomes more intense than the 964-cm^{-1} band in glasses with 2.6 mol% P_2O_5.

The P-free glass has two bands in the midfrequency region: a weak, narrow polarized band at 588 cm^{-1} and a broad partially depolarized weak band around 770 cm^{-1}. The 1.7-mol% and 2.6-mol% P_2O_5 glasses have a weak broad new band at 708 cm^{-1} of the HH spectrum.

In the low-frequency region (<500 cm^{-1}), the P_2O_5-free glass has a broad band at 490 cm^{-1} and a shoulder around 392 cm^{-1} (see also Domine and Piriou, 1986). The 490-cm^{-1} band loses intensity with respect to the band developing around 450 cm^{-1} in glasses with increasing P_2O_5 concentration.

The peraluminous glasses

The P_2O_5-free glass has two intense bands at 474 and 436 cm^{-1}, two weak bands at 590 and 786 cm^{-1}, and two broad, partially depolarized bands at 1030 and 1128 cm^{-1} (Fig. 3). With increasing P_2O_5, a relatively strong polar-

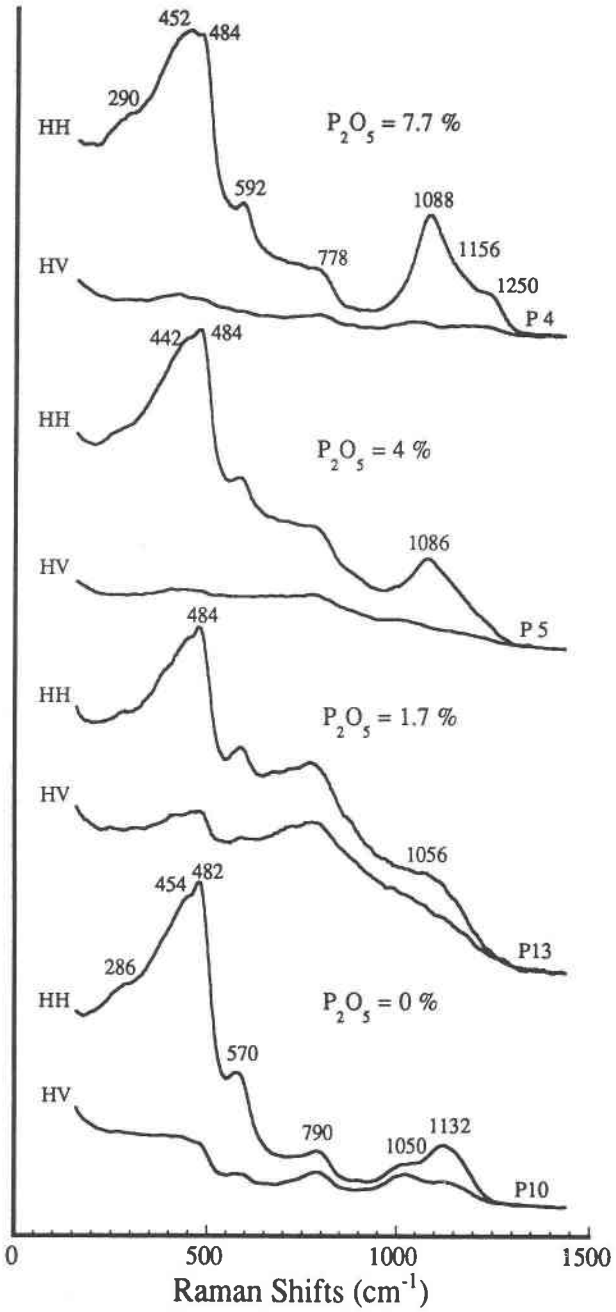

Fig. 4. The Raman spectra of subaluminous glasses. Samples P10 (P_2O_5 = 0%), P13 (P_2O_5 = 1.7%), P5 (P_2O_5 = 4%), P4 (P_2O_5 = 7.7%).

ized band at 1110 cm^{-1} replaces the two partially depolarized bands at 1030 and 1128 cm^{-1}. A new broad polarized band around 290 cm^{-1} grows in the low frequency region, and the intensity of the 474-cm^{-1} band increases relative to the 436-cm^{-1} band.

The subaluminous glasses

The Raman spectrum of the P-free subaluminous glass is similar to its peraluminous counterpart (Fig. 4). The most significant differences are the lower intensity of the 454-cm^{-1} band relative to the 482-cm^{-1} band and a more noticeable band at 570 cm^{-1}. As P_2O_5 increases, a strong polarized band grows at 1088 cm^{-1}.

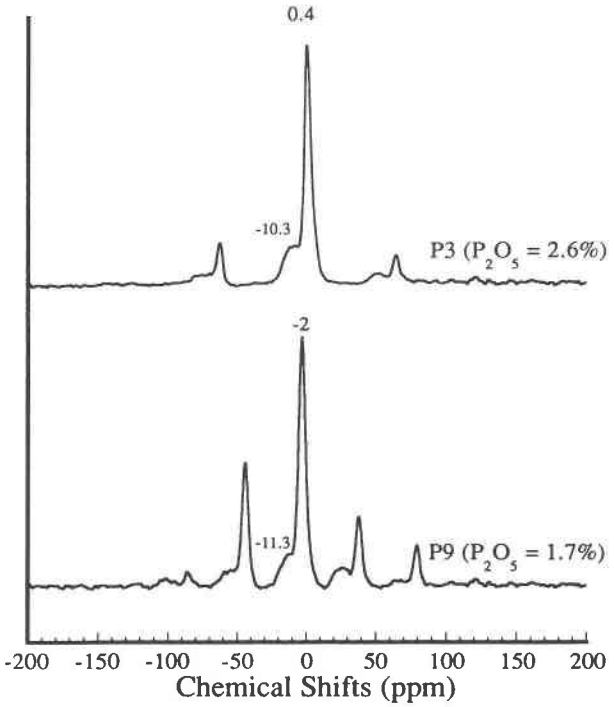

Fig. 5. The ^{31}P MAS NMR spectra of peralkaline glasses. Samples P9 (P_2O_5 = 1.7%), P3 (P_2O_5 = 2.6%).

The ^{31}P MAS NMR spectra

The ^{31}P MAS NMR spectra for peralkaline, peraluminous, and subaluminous glasses are illustrated in Figures 5, 6, and 7, respectively. The two peralkaline glasses have an intense peak near 0 ppm (0.4 to −2 ppm) and a shoulder near −11 ppm (−10.3 to −11.3 ppm). The peraluminous glasses have only one peak near −27 ppm. The chemical shift is not strongly influenced by P_2O_5 content. The spectra of the subaluminous glasses have only one peak, at about −20 to −22 ppm. The static NMR spectra are shown in Figures 8, 9, and 10 for the glasses within different K* regions and will be described and analyzed in the section discussing band assignment.

Raman and ^{31}P MAS NMR spectra of crystalline phosphates

Band assignments in the Raman and NMR spectra of glasses typically rely upon comparisons with the spectra of crystals of similar composition (e.g., Brawer and White, 1975; Dupree et al., 1988a). A number of observations suggests that certain high-frequency vibrational modes of silicate glasses, and glass in general, are highly localized, which in turn suggest that the high-frequency vibrational spectra of crystals and their corresponding glasses reflect the existence of similar structural units. The reader is referred to the papers of Brawer and White (1975), Fu-

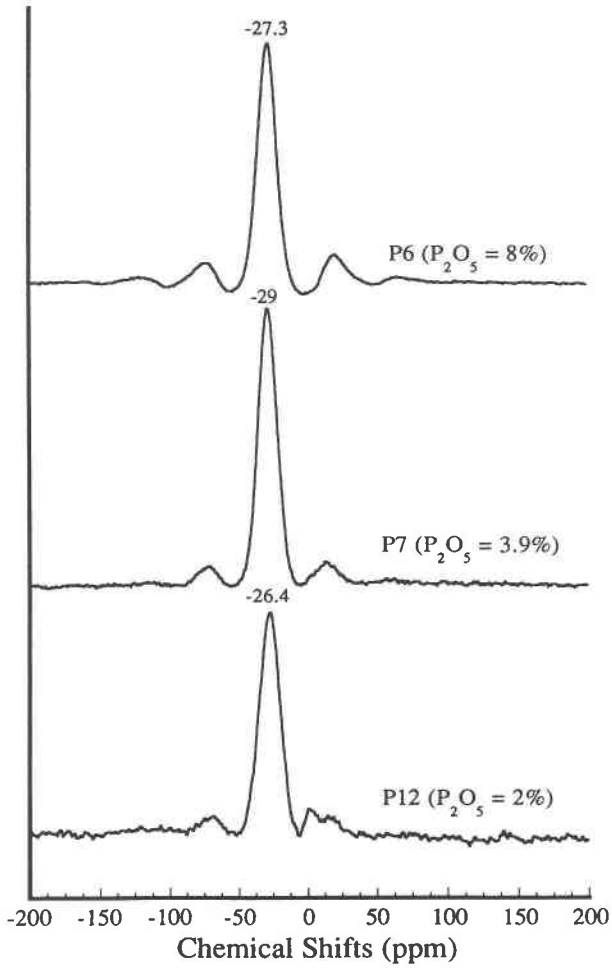

Fig. 6. The ^{31}P MAS NMR spectra of peraluminous glasses. Samples P12 (P_2O_5 = 2%), P7 (P_2O_5 = 3.9%), P6 (P_2O_5 = 8%).

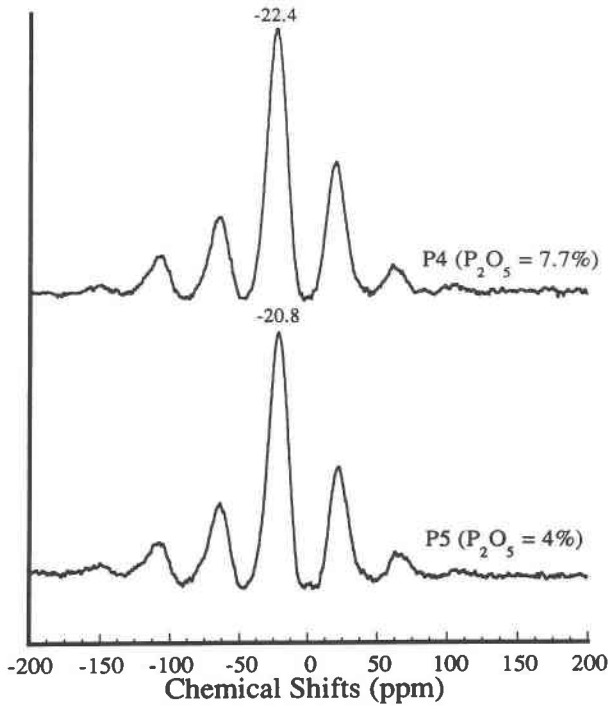

Fig. 7. The ^{31}P MAS NMR spectra of subaluminous glasses. Samples P5 (P_2O_5 = 4%), P4 (P_2O_5 = 7.7%).

rukawa et al. (1981), McMillan (1984), Dowty (1987), and Tallant and Nelson (1986) for comprehensive discussions of these questions. Low-frequency vibration modes, however, appear to be delocalized and present some difficulties in band assignment, since the nature of the vibrations responsible for these bands is not well understood. Systematic and detailed comparison of the spectra of series interrelated glasses suggests that even the low-frequency bands, however, are useful in identifying important structural features of glasses. More complete analyses of the low-frequency spectra are found in Matson et al. (1983), McMillan (1984), Mysen et al. (1985), and Domine and Piriou (1986).

The basic principle used in interpreting NMR chemical shifts is that the shielding of a given nuclei increases with the increasing ionicity of the bonds that the cation makes with nearest-neighbor O (Kirkpatrick, 1988). The chemical shift is also a function of the electron redistribution in these bonds caused by changes in next-nearest neighbors. These changes, however, are much smaller than those due to the primary coordination polyhedron. The application of MAS NMR to glasses, in general, has been reviewed by Kirkpatrick et al. (1986). Dupree et al. (1988a, 1988b, 1989) provide MAS NMR spectra of various phosphate-bearing glasses, as well as the spectra of some of their corresponding crystals.

In order to identify the Raman bands that are associated with P-O vibrations, spectra of three crystalline potassium phosphates were collected (Fig. 11). These include potassium orthophosphate (K_3PO_4), potassium pyrophosphate ($K_4P_2O_7$), and potassium metaphosphate (KPO_3). These compounds are listed in order of increasing polymerization of the PO_4 tetrahedron, i.e., from the monomer to dimer to infinite chain. They contain P^0, P^1, and P^2 phosphate tetrahedra, respectively, where the P^n notation identifies the number of POP (bridging) bonds per phosphate tetrahedron. The Raman spectra of crystalline phosphates show the following significant features: (1) The most intense peak in the high-frequency regions moves toward higher frequency with an increasing degree of polymerization of the phosphate tetrahedra. These peaks reflect the symmetric vibration of the KOP nonbridging bond (Tallant and Nelson, 1986). (2) The moderately intense peak near 700 cm^{-1} exists only in the dimer and more polymerized phosphates and is absent for the orthophosphate spectrum. This peak probably represents the symmetric vibration of the POP bridging bond (Tallant and Nelson, 1986).

The ^{31}P MAS NMR chemical shifts of these phosphates obtained from the literature are listed in Table 2. The chemical shifts are more shielded with increasing degrees of polymerization of the phosphate. Chemical shifts of

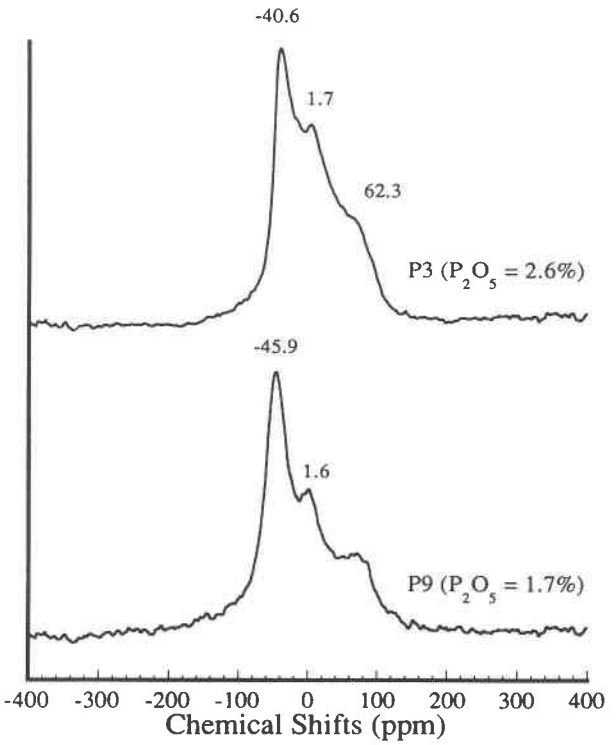

Fig. 8. The ^{31}P static NMR spectra of peralkaline glasses. Samples P9 (P_2O_5 = 1.7%), P3 (P_2O_5 = 2.6%).

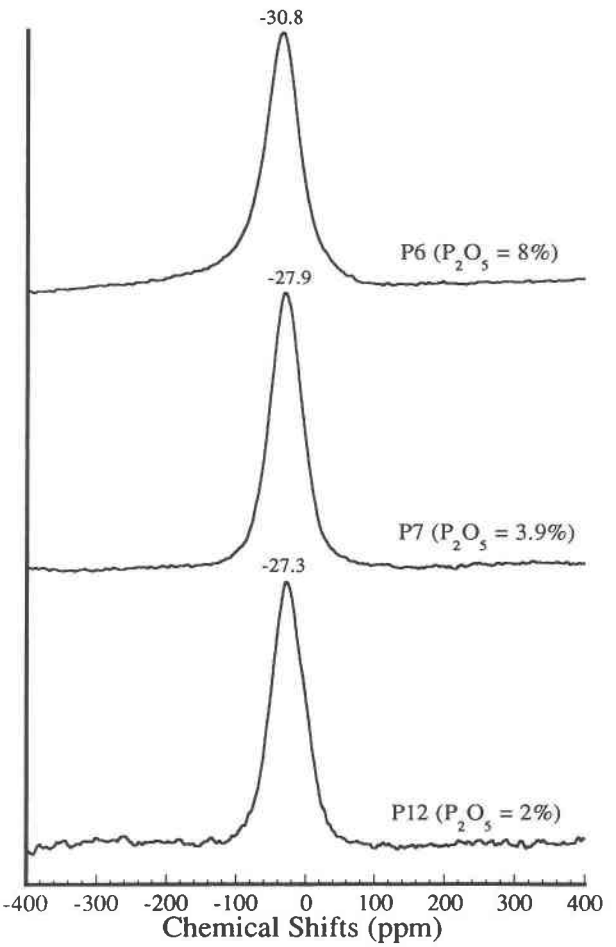

Fig. 9. The ^{31}P static NMR spectra of peraluminous glasses. Samples P12 (P_2O_5 = 2%), P7 (P_2O_5 = 3.9%), P6 (P_2O_5 = 8%).

$AlPO_4$ and SiP_2O_7 are also given in the same table, and other relevant phosphates will be cited in the text.

Band assignments

Bands in the peralkaline glasses

The most intense high-frequency Raman band (1090 cm^{-1}) in the P_2O_5-free glass is assigned to the symmetric stretching vibration of nonbridging O of Q^3 [generally, Q^n notation identifies the number (n) of SiOSi bridging bonds per silicate tetrahedron] and the intense low-frequency band (490 cm^{-1}) is assigned to the delocalized vibrations of the polymerized aluminosilicate network (Brawer and White, 1975; Virgo et al., 1980; Matson et al., 1983; McMillan, 1984). The bands near 704 and 1014 cm^{-1} gain intensity with increasing P_2O_5. These bands match the 715-cm^{-1} and 1015-cm^{-1} bands of the Raman spectra of crystalline pyrophosphate (Fig. 11), and therefore are assigned to pyrophosphate-type structural units in the melts. The band near 966 cm^{-1} exists only in P_2O_5-bearing glasses but loses intensity with increasing P_2O_5. The 966-cm^{-1} band is close to the intense 923-cm^{-1} band of crystalline orthophosphate (Fig. 11), although it is about 40 cm^{-1} higher. Nelson and Tallant (1984) observed a 940-cm^{-1} band in their Na_2O-P_2O_5-SiO_2 glasses that has the same wavenumber as the intense high-frequency band in crystalline Na_3PO_4. This band also loses intensity with increasing P_2O_5 content of the glass, as observed in our glasses. A 957-cm^{-1} band coexists with the 1010-cm^{-1} band in the Raman spectrum of the glass, where both orthophosphate and pyrophosphate species are identified by means of ^{31}P MAS NMR spectroscopy (Dupree et al., 1988a; see Fig. 12 and analysis in the NMR section below). The 964-cm^{-1} band, therefore, is assigned to the symmetric stretching vibration of nonbridging O (P^0) or orthophosphate tetrahedra.

The ^{31}P MAS NMR spectra only partially confirm the species we have identified in the Raman spectra of peralkaline glasses. The major peak observed in the 1.7-mol% and 2.6-mol% P_2O_5 glasses is close to the chemical shift of crystalline potassium pyrophosphate (−1.1 ppm, see Table 2). A small bump at −11 ppm coexists with −1.1 ppm peak in each of the two glasses. Its assignment will be discussed below. No chemical shifts corresponding to orthophosphate were observed.

The static ^{31}P NMR spectra were analyzed using the spectra of crystalline alkali phosphates (Duncan and Douglass, 1984). The 1.7-mol% and 2.6-mol% P_2O_5 glasses have an axial symmetry powder pattern (Harris, 1983) almost identical to that of crystalline $K_4P_2O_7$ (Dun-

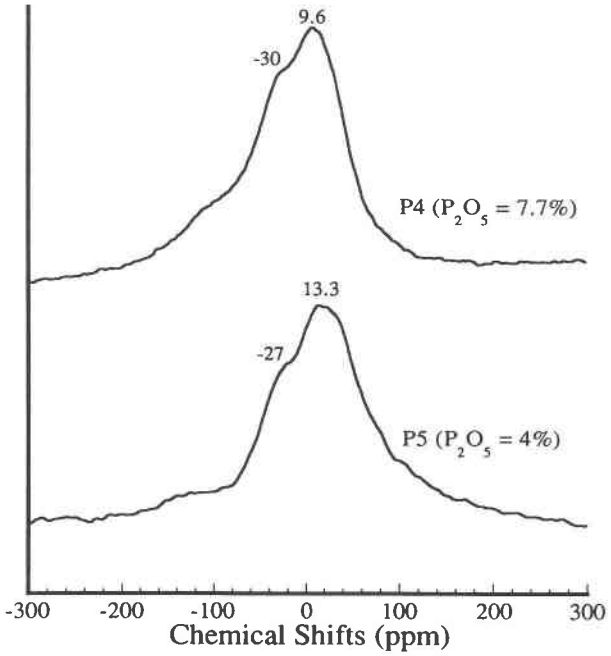

Fig. 10. The ^{31}P static NMR spectra of subaluminous glasses. Samples P5 (P_2O_5 = 4%), P4 (P_2O_5 = 7.7%).

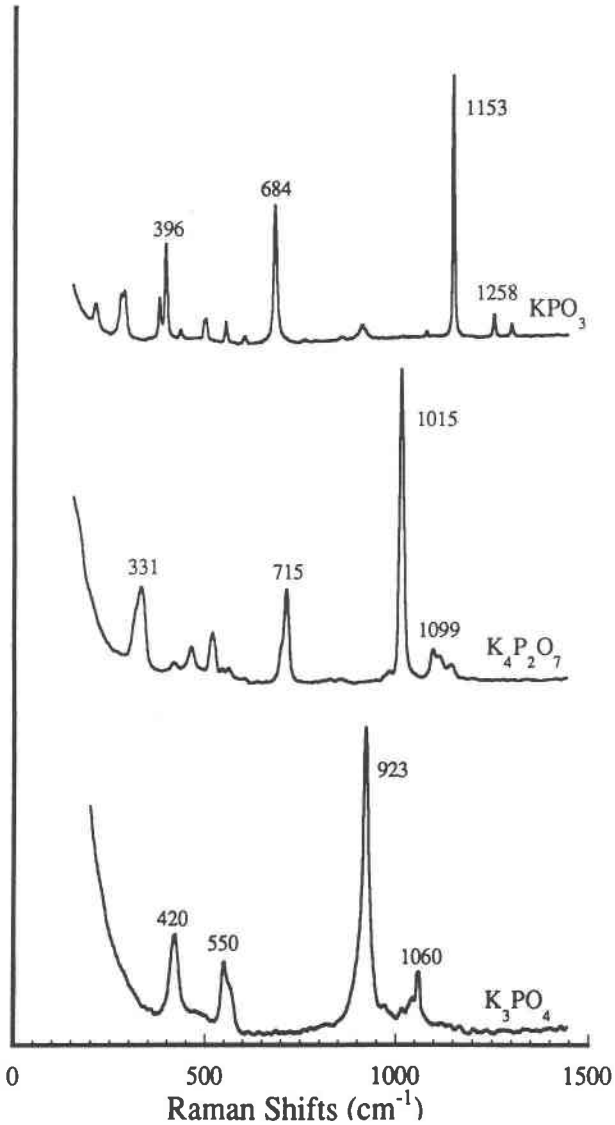

Fig. 11. The Raman spectra of crystalline potassium phosphates. Among them are orthophosphate (K_3PO_4), pyrophosphate ($K_4P_2O_7$), and metaphosphate (KPO_3).

can and Douglass, 1984) and that is consistent with the inferences from Raman and MAS ^{31}P NMR. A weak peak at 1.6 ppm occurs in both glasses but has a slightly greater intensity in the 2.6-mol% P_2O_5 glass. This peak overlaps the axial symmetry powder pattern of $K_4P_2O_7$ and seems related to the −11 ppm shoulder in MAS ^{31}P NMR of the same glasses. The MAS ^{31}P NMR spectra suggest that this P site (−11 ppm) is shielded more than that in pyrophosphate and is probably a chainlike phosphate species (Kirkpatrick, 1988; Dupree et al., 1989). The abundance of this species must be low, since its Raman band is buried under the strong KOSi(Q^3) band near 1100–1150 cm^{-1}. Nevertheless, it is clear that the static NMR profile of the 1.7-mol% and 2.6-mol% P_2O_5 glass is dominated by pyrophosphate species.

It is interesting to note that there is no ^{31}P chemical shift indicative of potassium orthophosphate in either the MAS or static NMR spectra. Yet the existence of this species in low P_2O_5 glasses is indicated by the 964-cm^{-1} Raman band. Since phosphate species have a strong scattering coefficient (Nelson and Tallant, 1984), it is possible for Raman spectra to show a much stronger signature of orthophosphate than the ^{31}P MAS NMR. To check this possibility, we collected the Raman spectrum of a P-bearing high potassium silicate glass from which Dupree et al. (1988a) obtained only a very weak orthophosphate and a very intense pyrophosphate chemical shift (Fig. 12).

TABLE 2. MAS ^{31}P NMR chemical shifts of crystals

K_3PO_4	$K_4P_2O_7$	$K_5P_3O_{10}$	KPO_3	$AlPO_4$	SiP_2O_7	P_2O_{10}
11.7*	−1.1**	−1.2, −4, −19*	−18.5, −19*	−25.3†	−33†	−46‡

* Grimmer and Haubenreisser (1983).
** Duncan and Douglass (1984).
† Bleam et al. (1989).
‡ Dupree et al. (1989).

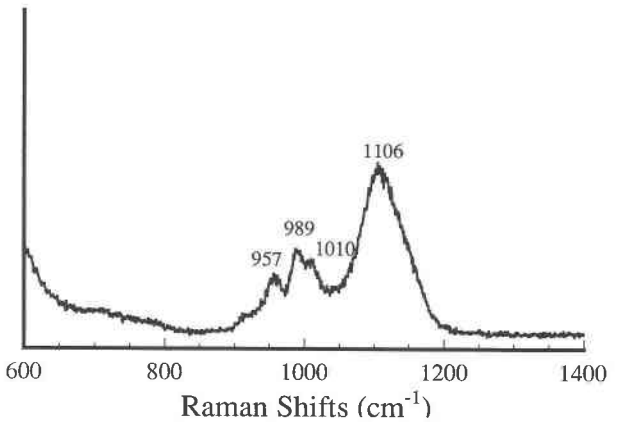

Fig. 12. The Raman spectrum of $32K_2O \cdot 5P_2O_5 \cdot 63SiO_2$ glass.

The Raman spectrum of the glass, nevertheless, shows a strong orthophosphate band at 957 cm^{-1} and a pyrophosphate band of slightly higher intensity at 1010 cm^{-1} (The 989-cm^{-1} band [$KOSi(Q^2)$] probably enhances the apparent intensity of 1010-cm^{-1} band). It seems that the proportion of orthophosphate species is greatly exaggerated in the Raman spectrum of the glass. Since the concentration of K_2O and P_2O_5 is much lower in our glasses than in those of Dupree et al., it is not extraordinary that the chemical shift for potassium orthophosphate species is absent or is concealed by the neighboring strong pyrophosphate peak. Although orthophosphate is only a minor species in these glasses, it is quite likely the dominant phosphate species at lower P concentrations (Dupree et al., 1988a).

Bands in the peraluminous glasses

The Raman spectrum of the P-free peraluminous glass is almost identical to those of SiO_2-Al_2O_3 (McMillan and Piriou, 1982). The addition of Al_2O_3 to SiO_2 glass and presumably the exchange of Al_2O_3 for K_2O in a subaluminous glass result in the development of a weak band near 1100 cm^{-1} and a loss of intensity of the sharp 480-cm^{-1} band relative to the 450-cm^{-1} band, which are believed to reflect the vibration of ≡SiOAl units (McMillan and Piriou, 1982).

P_2O_5-bearing glasses have two broad polarized bands at 1110 and 294 cm^{-1} that are not observed in the spectra of P_2O_5-free peraluminous glass (note that 1128-cm^{-1} band in P_2O_5-free glass is partially depolarized). The spectrum is compatible with a glass structure containing tetrahedrally coordinated $AlPO_4$ species. The dominant high-frequency band at 1108 cm^{-1} is observed in the spectra of crystalline $AlPO_4$ (berlinite) and in $AlPO_4$-SiO_2 glass (Kosinski et al., 1988). Moreover, the 294-cm^{-1} band is matched by a band near 300 cm^{-1} in the spectra of $AlPO_4$-SiO_2 glasses. A shoulder near 1200 cm^{-1} is observed also in the spectra of $AlPO_4$-SiO_2 glasses and as a weak band in berlinite (Kosinski et al., 1988). It is clear, therefore, that AlOP bonds similar to those in crystalline $AlPO_4$ characterize the peraluminous glasses.

The MAS and static ^{31}P NMR spectra confirm these assignments. Both spectra show single peaks from around −27 ppm (MAS) to around −28 ppm (static), consistent with the MAS of berlinite (−25 ppm) and the static spectra of amorphous $AlPO_4$ (−28 ppm). A shielding tensor of cubic symmetry is indicated by the static NMR powder pattern, in agreement with the cubic symmetric shielding tensor observed in crystalline and amorphous $AlPO_4$ (Kosinski et al., 1988).

Bands in the subaluminous glasses

The Raman spectrum of the P_2O_5-free subaluminous glass is similar to that of vitreous silica. The major differences in the Raman spectra between SiO_2-$KAlO_2$ and SiO_2 systems are the appearance of high-frequency bands caused by the vibration of SiOAl species and loss of intensity of the 450-cm^{-1} band relative to the 490-cm^{-1} band. The last two bands reflect the symmetrical stretch of the bridging O atom in SiOSi and $SiO^{[4]}Al$ bonds, respectively (McMillan et al., 1982). The $KOSi(Q^3)$ band is not observed. Therefore all K^+ act as charge-balancing cations for the $SiO^{[4]}Al$ bonds. The addition of P increases the intensity of the 450-cm^{-1} band (SiOSi) relative to the 490-cm^{-1} band ($SiO^{[4]}Al$) and produces a new band around 1090 cm^{-1}. The band near 1090 cm^{-1} has two possible origins: $AlPO_4$ and $KOSi(Q^3)$ both have major bands at this frequency. The increasing intensity of the 450-cm^{-1} band indicates the development of a Q^4-type SiOSi network that argues against the $KOSi(Q^3)$ assignment. Although there is no general agreement in the assignment of low-frequency Raman bands because of the delocalized nature of these vibrations, the consistent change of the low-frequency vibration envelope with chemical composition indicates that a gain in intensity of the 450-cm^{-1} band reflects the increasing degree of polymerization of the aluminosilicate network (Matson et al., 1983). This leaves $AlPO_4$ as the species responsible for the high-frequency band at 1088 cm^{-1}. Since alumina are incorporated in the aluminosilicate network together with K, the formation of AlOP bonds ($AlPO_4$ type) requires the breakdown of $KO^{[4]}Al$ bonds. This reaction is supported by the decreasing intensity of the 490-cm^{-1} band that is interpreted to be due to symmetrical stretching vibration of $SiO^{[4]}Al$ bonds in the silica-rich network (McMillan et al., 1982). The broad envelope from 1100 to 1250 cm^{-1} is difficult to interpret. Berlinite ($AlPO_4$) has a weak band at 1220 cm^{-1}, and the $AlPO_4$-bearing peraluminous glasses have a broad band near this frequency (Kosinski et al., 1988). Thus, some of the intensity of the 1250-cm^{-1} band may be caused by an $AlPO_4$ species. Crystalline KPO_3 has a major band near 1153 cm^{-1} and may also contribute energy in this range. The formation of KOP bonds is, in fact, required by mass balance to accommodate the K released from broken $KO^{[4]}Al$ bonds (see the discussion

section). It is concluded, therefore, that both $AlPO_4$ and potassium phosphate chains coexist in P-bearing subaluminous glasses. Additional evidence in support of this interpretation is given below.

The MAS ^{31}P NMR isotropic chemical shifts (−20 to −22 ppm) exclude the existence of SiP_2O_7-type and P_4O_{10}-type species that have chemical shifts near −35 and −46 ppm, respectively (Table 2). No ^{31}P MAS NMR data are available for $^{[4]}$SiOP-type species in glasses. However the lower coordination number of the Si atom tends to increase its bond order, which will in turn cause more shielding to ^{31}P nuclei (more negative in this case). Therefore, it is very unlikely that −20 ppm chemical shifts are caused by $^{[4]}$SiOP-type structural units. This implies that $KO^{[4]}Al$ bonds have to be broken to form new P-bearing species. The −20 to −22 ppm peaks are within the range of the chemical shift of KPO_3 (−19 ppm, Duncan and Douglass, 1984) and $AlPO_4$ (−25 ppm, Bleam et al., 1989). The FWHH of the −20 to −22 ppm peak is about 16 ppm, which could cover both the −19 and −25 ppm peaks. Thus, it is possible that the isotropic chemical shifts from KPO_3-type and $AlPO_4$-type structural units are combined into a single broad peak.

Molecules with similar isotropic chemical shifts could have a distinct symmetry of shielding tensors that appear different in the static ^{31}P NMR powder patterns. The static ^{31}P NMR spectra of the 4 and 8% P_2O_5 glasses have a prominent low-symmetry powder pattern that is very similar to that of $(NaPO_3)n$ (−148, 16, and 90 ppm; Duncan and Douglass, 1984). A strong shoulder around −29 ppm falls within the range of the $AlPO_4$ chemical shift. The static ^{31}P NMR of $AlPO_4$ in peraluminous glasses (Fig. 9) shows a single, isotropic, symmetrical peak at about −27 to −30 ppm. Therefore, the static ^{31}P NMR spectra can be modeled by combining the powder patterns of the shielding tensors of cubic symmetry ($AlPO_4$) and nonaxial symmetry (KPO_3), as deduced from MAS ^{31}P NMR.

Discussion

Solution model

The structure of the P-free peralkaline glass is relatively well understood. The role of K is that of a charge-balancing cation for AlO_4 tetrahedra and as a network-modifying cation for $KOSi(Q^3)$ tetrahedra. The silicate network is a solution of copolymerizing Q^3 and Q^4 silicate tetrahedra and charge-balanced AlO_4 tetrahedra (Engelhardt et al., 1985; Kirkpatrick et al., 1986; Domine and Piriou, 1986; McMillan et al., 1982; Mysen et al., 1981a). The addition of P causes significant modifications to the glass structure. P enters as variously polymerized phosphate tetrahedra using K as a network-modifying cation. The speciation of the potassium phosphates is controlled by the ratio of excess K (i.e., K in excess of that needed to charge balance the AlO_4 tetrahedra) over P; the lower the ratio, the more polymerized the phosphate species. Thus, phosphates exist first a monomers, then dimers, and then probably small chains as the P concentration is increased. In the process, P strips network-modifying K from $KOSi(Q^3)$ species, resulting in a higher state of polymerization of the aluminosilicate network. The increased degree of polymerization with increasing P_2O_5 in peralkaline silicate glasses was also observed by other researchers. Nelson and Tallant (1984) reported that addition of P_2O_5 to metasilicate (Q^2) glasses gives rise to a new Raman band characteristic of the symmetrical stretching vibration of NaOSi (Q^3). Dupree et al. came to the same conclusion by means of ^{29}Si MAS NMR spectroscopy (Dupree et al., 1988a): the resonance of Q^4 type structural units increases in intensity as P_2O_5 increases in peralkaline glasses. The occurrence of cristobalite in 7.6 mol% P_2O_5 peralkaline glass prepared for, but not analyzed, in this study is consistent with the above conclusions. Therefore, the homogeneous equilibria can be expressed as

$$\underset{(Q^3)}{2KOSi} + \underset{(P^3)}{POP} = \underset{(P^0,P^1)}{2KOP} + \underset{(Q^4)}{SiOSi} \qquad (1)$$

where P^n refers to PO_4 tetrahedra containing n POP bridging bonds. The phosphate species must largely reside outside the aluminosilicate network, as there is no evidence for the existence of Si and P bonding in the MAS ^{31}P NMR spectrum (see also Nelson and Tallant, 1984; Dupree et al., 1988a).

The structural role of excess Al in peraluminous melts has been a topic of considerable debate (e.g., Lacey, 1968; Mysen et al., 1980, 1981a; McMillan and Piriou, 1982; Sato et al., 1991). It has been concluded that tetrahedrally coordinated Al is the primary structural unit for Al in subaluminous to moderately peraluminous melts. Fivefold coordinated Al is observed only as a minor species coexisting with the fourfold coordinated Al in $15CaO35Al_2O_350SiO_2$ glass ($Al_2O_3/CaO = 2.3$; Sato et al., 1991). For glasses with an even higher Al_2O_3/CaO ratio (7.6 to 12.2), the data from ^{27}Al MAS NMR suggest that a portion of the Al is in highly distorted sites in addition to the four-, five-, and sixfold coordinated sites (Sato et al., 1991). The Al_2O_3/CaO ratios of the peraluminous glasses of this study are less than or equal to 2.3, and the low excess Al_2O_3/SiO_2 ratios (<0.13) of the glasses would also stabilize Al in tetrahedral sites (Risbud et al., 1987). It is concluded, therefore, that excess Al is primarily located in tetrahedral sites in the peraluminous melts and it forms triclusters with or without SiO_4 units (noted as AlOSi and AlOAl for "with" and "without," respectively, in the following).

P_2O_5 reacts with excess Al in peraluminous melts to form $AlPO_4$ species. If the excess Al exists as triclusters containing silicate tetrahedra, then the homogeneous equilibrium is

$$2AlOSi + POP = 2AlOP + SiOSi \qquad (2)$$

where the formation of AlOP units results in the polymerization of the silicate network. Alternatively, if the

excess Al exists outside the silicate network, then the homogeneous equilibrium is

$$\text{AlOAl} + \text{POP} = 2\text{AlOP}. \quad (3)$$

Reaction 2 may be indicated by the increase in intensity of the 475-cm^{-1} band, which is believed to reflect the vibrations of bridging O in the aluminosilicate network (McMillan and Piriou, 1982).

One question raised about the above two reactions is whether AlOP bonds reside within the aluminosilicate network, forming Si-O-Al-O-P-O type species, or outside the network, as a separate species. It has been argued that there is no independent MAS NMR data for the isotropic chemical shift of the species Si-O-Al-O-P-O in crystal or glasses, thereby, rendering our previous ^{31}P MAS NMR discussion less convincing. There is not yet a general agreement on this. The analysis of vibrational spectra yields different interpretations. Mysen et al. (1981b) and Tallant and Nelson (1986) argued against the existence of such a species because of the absence of the SiOP Raman band, which is highly localized in the high-frequency region. However, Mysen's conclusion is based on somewhat subjective deconvolution analysis, and the glasses of Tallant and Nelson are far too low in SiO_2 concentration to be compared to this study. In contrast, Kosinski et al. (1988) argued for the Si-O-Al-O-P-O type structural units in glass of $50SiO_2$-$25Al_2O_3$-$25P_2O_5$ based on the similarity of Raman spectra between the glass and vitreous silica. Considering the ambiguity involved in the interpretation of Raman spectra, it is possible that ^{31}P static NMR spectra may offer clues to the correct model. If Si-O-Al-O-P-O type species exist, the cubic symmetry of the shielding tensor of $AlPO_4$-type species will be demoted to a lower symmetry, a result which should be resolved in the static spectra. This is not observed; the static ^{31}P NMR spectra has the expected cubic symmetry (Fig. 9). For this reason, it is thus concluded that $AlPO_4$ species reside mostly outside the aluminosilicate network. This does not exclude the existence of a small number of P-O-Si species, which certainly are predicted from thermodynamic considerations.

P-free subaluminous melts are composed of fully polymerized aluminate-silicate networks in which all K cations are incorporated into $KAlO_4$ complexes as charge-balancing cations, noted here as $KO^{[4]}Al$ (Sharma et al., 1978; Virgo et al., 1979; Mysen et al., 1980, 1981a, 1982; McMillan et al., 1982; Sato et al., 1991). In analyzing the structures of peralkaline and peraluminous melts, it is clear that $KO^{[4]}Al$ bonds are very strong compared with $KOSi(Q^3)$ and AlOSi or AlOAl bonds. Once KOSi, AlOSi, or AlOAl bonds are eliminated, P_2O_5 must obtain K and Al from the strong $KO^{[4]}Al$ species. The major difference between subaluminous melts and P_2O_5-rich peralkaline or peraluminous melts is that the charge-balanced subaluminous melts contain only $KO^{[4]}Al$ species, even at the lowest P_2O_5 contents, and potassium phosphates or aluminophosphate are not present when P_2O_5 is required to break the $KO^{[4]}Al$ bonds. Therefore it is energetically favorable and stoichiometrically feasible for the first phosphate species to have a low K/P (or Al/P) ratio. The product is therefore metaphosphate (K/P = 1) in subaluminous melts instead of orthophosphate (K/P = 4), as in low P_2O_5 peralkaline melts. The homogeneous equilibrium describing this process is

$$KAlO_2 + P_2O_5 = KPO_3 + AlPO_4 \quad (4)$$

where $AlPO_4$ species rather than the less stable AlOSi species are formed. The intensity of the 450-cm^{-1} Raman band increases relative to the 480-cm^{-1} band because part of the $KO^{[4]}Al$ bonds are eliminated. $KO^{[4]}Al$ bonds depress the 450-cm^{-1} bands of SiOSi vibration in vitreous SiO_2 (McMillan and Piriou, 1982). Since P_2O_5 is evenly shared by potassium metaphosphate and $AlPO_4$-type aluminophosphate (see Reaction 4), the abundance of each species is roughly half of those similar species in other melts with the same amount of P_2O_5. This explains the relatively low intensities of the KOP and AlOP bonds in the Raman spectra of subaluminous melts.

Applications

The solution behavior of P in silicate melts is rich in complexity. The activity coefficient of P is smaller in silicate melts that contain network-modifying cations appropriate to form stable phosphate complexes. Excess alkalis perform this function in peralkaline melts, excess Al in peraluminous melts, and mainly divalent cations in metaluminous melts. This model explains a number of interesting experimental observations.

1. The addition of P_2O_5 to multisaturated liquids (e.g., enstatite-forsterite, cristobalite-enstatite) shifts the boundary curves to lower SiO_2 contents, thereby increasing the γ_{SiO_2} in the liquids (Kushiro, 1975). This is consistent with the homogeneous equilibrium

$$2\text{MgOSi} + \text{POP} = 2\text{MgOP} + \text{SiOSi} \quad (5)$$

in which the production of MgOP complexes causes the silicate network to polymerize (Hess, 1980; Ryerson and Hess, 1980). The role of P, therefore, is to increase the activity coefficient of SiO_2 but to lower the activity coefficient of selected network-modifying cations. Conversely, the activity coefficient of P is lowest in silicate melts that contain the highest concentration of network-modifying cation. This factor explains why the solubilities of apatite and whitlockite are greatest in mafic to ultramafic melts rich in network-modifying cations and least in nearly subaluminous granitic melts under identical temperatures and pressures (Watson, 1979; Hess et al., 1989; Dickinson and Hess, 1983).

2. The solubility of $LaPO_4$ (monazite structure) exhibits both a peralkaline and peraluminous effect in anhydrous potassium aluminosilicate melts (Ellison and Hess, 1988). The solubility is at a minimum in the subaluminous melts because the free energy change of the reaction

$$KAlO_2 + P_2O_5 = KPO_3 + AlPO_4 \quad (6)$$

is not as favorable as the free energy changes of the re-

actions in peraluminous and peralkaline melts (see Eqs. 2 and 1). The reason for this observation, of course, is that P must attack the very stable $KAlO_2$ complex in subaluminous melts but has easy access to the relatively less stable excess Al and excess K complexes in other melts. It is noteworthy that the monazite peralkaline effect is seen also in hydrous melts (Montel, 1986), demonstrating that the homogeneous equilibrium

$$2SiOH + POP = 2POH + SiOSi \quad (7)$$

does not have a significant role in stabilizing P_2O_5. This conclusion is consistent with the relatively constant solubility of apatite in anhydrous and H_2O-saturated granitic melts (Green and Watson, 1982).

3. The strong peraluminous effect on P and the strong association of P and rare earth elements (Ryerson and Hess, 1978) suggest that P has a strong affinity for M^{3+}. Indeed, the addition of P increases the Fe^{3+}/Fe^{2+} redox ratios in peraluminous melts and implies the formation of $Fe^{3+}PO_4$ complexes (Dickenson and Hess, 1983; Gwinn and Hess, 1992). BOP complexes in peraluminous melts are also anticipated (Gan and Hess, unpublished work). The high P_2O_5 contents of peraluminous pegmatites relative to high silica rhyolites are likely to be a consequence of the formation of BPO_4 complexes (London, 1987). Crystal-liquid partition coefficients of other trivalent cations such as Sc^{3+}, Ga^{3+}, and Y^{3+}, among others, should be sensitive to the P_2O_5 contents of silicate melts.

The solubilities of high field-strength cations (Zr^{4+}, Ti^{4+}, etc.) in high silica melts strongly depend on the availability of network-modifying cations (e.g., K^+, Ca^{2+}). P^{5+} joins in the competition for network-modifying cations, and therefore reduces their availability to other high field-strength cations, thus changing their solubilities. How P_2O_5 competes with other high field-strength cations for a limited number of network-modifying cations is a question that cannot yet be addressed. The establishment of a hierarchy of such interactions is an important goal in the characterization of the solution properties of highly charged trace elements.

Acknowledgments

We wish to acknowledge the generous use of the spectrometers of Bill Risen in the Department of Chemistry and of Phil Bray in the Department of Physics at Brown University. Thanks also to Jim Kirkpatrick for his assistance in getting additional NMR spectra. H.G. thanks George Tsagaropoulos for his help in using the Raman spectrometer. We also thank Jim Dickinson of Corning Glass for supplying us with most of the glasses and R.K. Brow and two anonymous referees for reviews of the manuscript. Finally, we express our gratitude to the National Science Foundation for their generous financial support (grants EAR-8719358, EAR-9017790).

References cited

Bleam, W.F., Pfeffer, P.E., and Frye, J.S. (1989) ^{31}P solid state nuclear magnetic resonance spectroscopy of aluminum phosphate minerals. Physics and Chemistry of Minerals, 16, 455–464.

Brawer, S.A., and White, W.B. (1975) Raman spectroscopic investigation of the structure of silicate glasses I. The binary alkali silicates. Journal of Chemical Physics, 63, 2421–2432.

——— (1977) Raman spectroscopic study of hexavalent chromium in some silicate and borate glasses. Materials Research Bulletin, 12, 281–288.

Dickenson, M.P., and Hess, P.C. (1981) Redox equilibria and the structural role of iron in aluminosilicate melts. Contributions to Mineralogy and Petrology, 78, 352–357.

——— (1983) Fe redox equilibria and the structural role of P^{5+}, Ti^{4+} and Fe^{3+}. Eos, 64, 350.

——— (1986) The structural role and homogeneous redox equilibria of iron in peraluminous, metaluminous and peralkaline silicate melts. Contributions to Mineralogy and Petrology, 92, 207–217.

Dickinson, J.E., and Hess, P.C. (1983) Role of whitlockite and apatite in lunar felsite (abs.). Lunar and Planetary Science, 14, 158.

——— (1985) Rutile solubility and titanium coordination in silicate melts. Geochimica et Cosmochimica Acta, 49, 2289–2296.

Domine, F., and Piriou, B. (1986) Raman spectroscopic study of the SiO_2-Al_2O_3-K_2O vitreous system: Distribution of silicon and second neighbors. American Mineralogist, 71, 38–50.

Dowty, E. (1987) Vibrational interactions of tetrahedra in silicate glasses and crystals: II. Calculations on melilites, pyroxenes, silica polymorphs and feldspars. Physics and Chemistry of Minerals, 14, 122–138.

Duncan, T.M., and Douglass, D.C. (1984) On the ^{31}P chemical shift anisotropy in condensed phosphates. Chemical Physics, 87, 339–349.

Dupree, R., Holland, D., and Mortuza, M.G. (1988a) The role of small amounts of P_2O_5 in the structure of alkali disilicate glasses. Physics and Chemistry of Glasses, 29, 18–21.

Dupree, R., Holland, D., Mortuza, M.G., Collins, J.A., and Lockyer, M.W.G. (1988b) An MAS NMR study of network-cation coordination in phosphosilicate glasses. Journal of Non-Crystalline Solids, 106, 403–407.

——— (1989) Magic angle spinning NMR of alkali phospho-aluminosilicate glasses. Journal of Non-Crystalline Solids, 112, 111–119.

Ellison, A., and Hess, P.C. (1988) Peraluminous and peralkaline effects upon "monazite" solubility in high-silica liquids. Eos, 69, 498.

——— (1989) Solution properties of rare earth elements in silicate melts: Inference from immiscible liquids. Geochimica et Cosmochimica Acta, 53, 1965–1974.

Englehardt, G., Nofz, M., Forkel, K., Wihsmann, F.G., Magi, M., Samoson, A., and Lippman, E. (1985) Structural studies of calcium aluminosilicate glasses by high resolution solid static ^{29}Si and ^{27}Al magic angle spinning nuclear magnetic resonance. Physics and Chemistry of Glasses, 26, 157–165.

Furukawa, T., Fox, K.E., and White, W.B. (1981) Raman spectroscopic investigation of the structure of silicate glasses. III. Raman intensities and structural units in sodium silicate glasses. Journal of chemical Physics, 15, 3226–3237.

Green, T.H., and Watson, E.B. (1982) Crystallization of apatite in natural magmas under high pressure hydrous condition, with particular reference to orogenic rock series. Contributions to Mineralogy and Petrology, 79, 96–105.

Grimmer, A.R., and Haubenreisser, U. (1983) High-field static and MAS ^{31}P NMR: Chemical shift tensors of polycrystalline potassium phosphates $P_2O_5 \cdot xK_2O$ ($0 < x < 3$). Chemical Physics Letters, 99, (5–6), 487–490.

Gwinn, R., and Hess, P.C. (1989) Iron and titanium solution properties in peraluminous and peralkaline rhyolitic liquids. Contributions to Mineralogy and Petrology, 101, 326–338.

——— (1992) The role of phosphorus in rhyolitic liquids as determined from the homogeneous iron redox equilibria. Contributions to Mineralogy and Petrology, in press.

Harris, R.K. (1983) Nuclear magnetic resonance spectroscopy. Pitman, Marshfield, Massachusetts.

Hess, P.C. (1980) Polymerization model for silicate melts. In R.B. Hargraves, Ed., Physics of magmatic processes, p. 1–48. Princeton University Press, Princeton, New Jersey.

Hess, P.C., Horzempa, P., and Rutherford, M.J. (1989) Fractionation of Apollo 15 KREEP basalts (abs.). Lunar and Planetary Science, 20, 408–409.

Kirkpatrick, R.J. (1988) MAS NMR spectroscopy of minerals and glasses. In Mineralogical Society of America Reviews in Mineralogy, 18, 341–403.

Kirkpatrick, R.J., Dunn, T., Schramm, S., Smith, K.A., Oestrike, R., and

Turner, F. (1986) Magic-angle sample-spinning nuclear magnetic resonance spectroscopy of silicate glasses: A review. In G.E. Walrafen and A.G. Revesz, Eds., Structure and bonding in noncrystalline solids, p. 303–327. Plenum Press, New York.

Kosinski, S.G., Krol, D.M., Duncan, T.M., Douglass, D.C., MacChesney, J.B., and Simpson, J.R. (1988) Raman and NMR spectroscopy of SiO_2 glasses co-doped with Al_2O_3 and P_2O_5. Journal of Non-Crystalline Solids, 105, 45–52.

Kushiro, I. (1975) On the nature of silicate melts and its significance in magma genesis: Regularities in the shift of liquid boundaries involving olivine, pyroxene, and silica minerals. American Journal of Science, 275, 411–431.

Lacey, E.D. (1968) Configurational change in silicates with particular reference to network structures. Acta Crystallographica, 18, 141–150.

London, D. (1987) Internal differentiation of rare element pegmatites: Effects of boron, phosphorus and fluorine. Geochimica et Cosmochimica Acta, 51, 403–420.

Matson, D.W., Sharma, S.K., and Philpotts, J.A. (1983) The structure of high-silica alkali-silicate glasses—A Raman spectroscopic study. Journal of Non-Crystalline Solids, 58, 323–352.

McMillan, P. (1984) Structural studies of silicate glasses and melts—Applications and limitations of Raman spectroscopy. American Mineralogist, 69, 622–644.

McMillan, P., and Piriou, B. (1982) The structures and vibrational spectra of crystals and glasses in the silica-alumina system. Journal of Non-Crystalline Solids, 53, 279–298.

McMillan, P., Piriou, B., and Navrotsky, A. (1982) A Raman spectroscopic study of glasses along the joins silica-calcium aluminate, silica-sodium aluminate, and silica-potassium aluminate. Geochimica et Cosmochimica Acta, 46, 2021–2037.

Montel, J.-C. (1986) Experimental determination of the solubility of Cemonazite in SiO_2-Al_2O_3-K_2O-Na_2O melts at 800 °C, 2 Kb, under H_2O-saturated conditions. Geology, 14, 659–662.

Mysen, B.O., Virgo, D., and Scarf, C.M. (1980) Relations between the anionic structure and viscosity of silicate melts, a Raman spectroscopic study. American Mineralogist, 65, 690–710.

Mysen, B.O., Virgo, D., and Kushiro, I. (1981a) The structural role of aluminum in silicate melts—a Raman spectroscopic study at 1 atmosphere. American Mineralogist, 66, 678–701.

Mysen, B.O., Ryerson, F.J., and Virgo, D. (1981b) The structural role of phosphorus in silicate melts. American Mineralogist, 66, 106–117.

Mysen, B.O., Virgo, D., and Seifert, F.A. (1982) The structure of silicate melts: Implications for chemical and physical properties of natural magma. Reviews of Geophysics, 20, 353–383.

——— (1985) Relationship between properties and structure of aluminosilicate melts. American Mineralogist, 69, 834–847.

Naski, G., and Hess, P.C. (1985) SnO_2 solubility: Experimental results in peraluminous and peralkaline high silica glasses. Eos, 66, 412.

Nelson, C., and Tallant, D.R. (1984) Raman studies of sodium silicate glasses with low phosphate contents. Physics and Chemistry of Glasses, 25, 31–38.

Nelson, C., Furukawa, T., and White, W.B. (1983) Transition metal ions in glasses: Network modifiers or quasi-molecular complexes. Materials Research Bulletin, 18, 959–966.

Risbud, S.H., Kirkpatrick, R.J., Taglialavore, A.P., and Montez, B. (1987) Solid state NMR evidence for 4-, 5-, and 6-fold aluminum sites in roller-quenched SiO_2-Al_2O_3 glasses. Journal of American Ceramic Society, 70, C10–C12.

Ryerson, F.J., and Hess, P.C. (1978) Implications of liquid-liquid distribution coefficients to mineral-liquid partitioning. Geochimica et Cosmochimica Acta, 42, 921–932.

——— (1980) The role of P_2O_5 in silicate melts. Geochimica et Cosmochimica Acta, 44, 611–624.

Sato, R.K., McMillan, P.F., Dennison, P., and Dupree, R. (1991) A structural investigation of high alumina glasses in the CaO-Al_2O_3-SiO_2 system via Raman and magic angle spinning nuclear magnetic resonance spectroscopy. Physics and Chemistry of Glasses, 33, 149–156.

Sharma, S.K., Virgo, D., and Mysen, B.O. (1978) Structure of glasses and melts of $Na_2O \cdot xSiO_2$ (x = 1, 2, 3) composition from Raman spectroscopy. Carnegie Institution of Washington Year Book, 77, 649–652.

Tallant, D.R., and Nelson, C. (1986) Raman investigation of glass structure in the Na_2O-SiO_2-P_2O_5-Al_2O_3 system. Physics and Chemistry of Glasses, 27 (2), 75–79.

Verweij, H. (1981) Raman study of arsenic-containing potassium silicate glasses. Journal of the American Ceramic Society, 64, 493–498.

Virgo, D., Seifert, F., and Mysen, B.O. (1979) Three dimensional network structures of glasses in the systems $CaAl_2O_4$-SiO_2, $NaAlO_2$-SiO_2, $NaFeO_2$-SiO_2, and $NaGaO_2$-SiO_2 at 1 atm. Carnegie Institution of Washington Year Book, 78, 506–511.

Virgo, D., Mysen, B.O., and Kushiro, I. (1980) Anionic constitution of silicate melts quenched at 1 atm from Raman spectroscopy: Implications for the structures of igneous melts. Science, 208, 1371–1373.

Visser, W., and Koster van Groos, A.F. (1979) Effects of P_2O_5 and TiO_2 on the liquid-liquid equilibria in the system K_2O-FeO-Al_2O_3-SiO_2. American Journal of Science, 279, 970–989.

Watson, E.B. (1976) Two liquid partition coefficients: Experimental data and geochemical implications. Contributions to Mineralogy and Petrology, 56, 119–134.

——— (1979) Zircon saturation in felsic liquids: Experimental data and applications to trace element geochemistry. Contributions to Mineralogy and Petrology, 70, 407–419.

Wyllie, P.J., and Tuttle, D.F. (1964) Experimental investigation of silicates systems containing two volatile components. III. The effects of SO_3,P_2O_5, HCl and Li_2O in addition to H_2O on the melting temperatures of albite and granite. American Journal of Science, 262, 930–939.

Manuscript received April 18, 1991
Manuscript accepted January 6, 1992